NBSIR 73-413

Measurement of Depth-Dose Distributions in Carbon, Aluminum, Polyethylene, and Polystyrene for 10-MEV Incident Electrons

J. C. Humphreys, S. E. Chappell, W. L. McLaughlin, and R. D. Jarrett

Applied Radiation Division
Center for Radiation Research
Institute for Basic Standards
National Bureau of Standards
Washington, D. C. 20234

November 1973

Interim Report

Prepared for
Food Laboratory
U. S. Army Natick Laboratories
Natick, Massachusetts 01760

NBSIR 73-413

MEASUREMENT OF DEPTH-DOSE DISTRIBUTIONS IN CARBON, ALUMINUM, POLYETHYLENE, AND POLYSTYRENE FOR 10-MEV INCIDENT ELECTRONS

J. C. Humphreys, S. E. Chappell, W. L. McLaughlin, and R. D. Jarrett

Applied Radiation Division
Center for Radiation Research
Institute for Basic Standards
National Bureau of Standards
Washington, D. C. 20234

November 1973

Interim Report

This report is to be superseded by a future publication which will receive general distribution and should be cited as a reference. Please consult the NBS Office of Technical Information and Publications to obtain the proper citation.

Prepared for
Food Laboratory
U. S. Army Natick Laboratories
Natick, Massachusetts 01760

U. S. DEPARTMENT OF COMMERCE, Frederick B. Dent, Secretary

NATIONAL BUREAU OF STANDARDS, Richard W. Roberts, Director

ABSTRACT

Depth-dose distributions of 10-MeV electrons incident on homogeneous media of carbon, aluminum, polyethylene, and polystyrene have been measured using thin radiochromic dye-film dosimeters. Two types of dye-film dosimeters were employed as "cavities" within the media in two different geometrical configurations. One configuration was a stack with the dosimeters interleaved between disks of the medium and placed perpendicular to the incident electron beam direction. The other configuration was a wedge assembly with a single piece of dye film placed between pieces of the medium at a small angle to the beam direction. The results show no significant difference between dosimeter type or experimental arrangement. In addition, good agreement is shown in comparisons of experimental and Monte Carlo calculated depth-dose distributions characterized by such parameters as extrapolated range, depth of peak dose, and ratio of peak to entrance dose.

Key Words: Aluminum; carbon; depth dose; depth-dose distributions; dye-film dosimeters; polyethylene; polystyrene; radiochromic dyes; 10-MeV electrons

TABLE OF CONTENTS

Page

ABSTRACT..... ii

LIST OF FIGURES..... iv

LIST OF TABLES..... vi

A. INTRODUCTION..... 1

B. EXPERIMENTAL METHOD..... 4

B.1. Description of the Irradiation Facilities..... 4
B.2. Material-Dosimeter Arrangements Under Irradiation..... 6
B.3. Optical Density Measurements..... 8

C. RESULTS..... 14

C.1. Calibration of the Dosimeters..... 14
C.2. A Comparison of Dose Rates of the NBS and Natick Laboratories ^{60}Co γ-ray Sources..... 18
C.3. Depth-Dose Distributions in Electron Irradiated Materials..... 20

D. CONCLUSIONS..... 36

D.1. Comparison of Experimental Results with Theory..... 36
D.2. Comparison of Nominal and Experimental Entrance Doses..... 38
D.3. Comparison of Tissue and Near Tissue-Equivalent Materials..... 40
D.4. Possible Negative Effects on Results by Some Experimental Conditions..... 42
D.5. Suggestions for Future Experiments..... 43

REFERENCES..... 44

LIST OF FIGURES

		Page
1.	Schematic diagram of the NBS ^{60}Co pool source, and dye film holder.	5
2.	"Wedge" method of mounting dye-film dosimeters in homogeneous medium; (a) electron beam direction is parallel to page, (b) electron beam direction is perpendicular to page.	7
3.	Optical absorption spectrum of film type A, irradiated and unirradiated.	10
4.	Optical absorption spectrum of film type B, irradiated and unirradiated.	11
5.	^{60}Co γ-ray calibration curves of film type A in air or nitrogen atmosphere. Optical densities measured at two wavelengths.	15
6.	^{60}Co γ-ray calibration curves of film type B in air. Optical densities measured at two wavelengths.	16
7.	10-MeV electron depth-dose distributions in carbon and aluminum measured with film type A.	22
8.	10-MeV electron depth-dose distributions in polystyrene and polyethylene measured with film type A.	23
9.	10-MeV electron depth-dose distributions in carbon measured with film type B.	24
10.	10-MeV electron depth-dose distributions in aluminum measured with film type B.	25
11.	10-MeV electron depth-dose distributions in polystyrene measured with film type B.	26

Page

12. 10-MeV electron depth-dose distributions in polyethylene measured with film type B. 27

13. Experimental and calculated 10-MeV electron depth-dose distributions in carbon and aluminum. 30

LIST OF TABLES

		Page
1.	Comparison of Dose Rates of the NBS and Natick Laboratories ^{60}Co γ-ray Sources	19
2.	Electron Mass Collision Stopping Power Ratios, Material to Film	28
3.	Comparison of Some Experimental and Calculated Depth-Dose Parameters for the Different Materials	31
4.	Peak and Entrance Doses of Depth-Dose Distributions	33
5.	Comparison of Results of the "Stack" and "Wedge" Methods of Depth-Dose Measurements	34
6.	Comparison of Experimental and Calculated Depth-Dose Parameters for Carbon and Aluminum	37
7.	Entrance Dose in Water from Experimental Dose in Media: Comparison of Experimental and Nominal Entrance Doses	39
8.	Experimental and Calculated Depth-Dose Parameters of Tissue and Near Tissue-Equivalent Materials for 10-MeV Electrons	41

A. INTRODUCTION

The purpose of this study is to determine energy-deposition profiles, or depth-dose distributions, which result from the irradiation of homogeneous materials by high-energy electrons. The data obtained in this study will have wide application. Some examples of its use are to provide basic data for such areas as medical therapy and the radiation processing of materials.

Detailed depth-dose distributions in the irradiated media were determined by means of thin dye-film dosimeters. These dosimeters, in effect, were small, solid-filled "cavities" in the irradiated materials. The theory and use of such cavities in radiation dosimetry has been thoroughly investigated and is well understood. In general, the cavities may be filled with any material in a gaseous, liquid, or solid state [1]*. Several investigators have reported previously the successful use of dye-film dosimeters in applications in which materials were irradiated by broad, spatially uniform electron beams with energies up to 3 MeV [2-7]. The experimental results were compared successfully with Monte Carlo calculations which predicted the depth-dose distributions.

Two different thin dye-film dosimeters were employed in this study. They were hexahydroxyethyl pararosaniline cyanide in nylon (film type A)

---

*Figures in brackets indicate the literature references which are listed at the end of this report.

and malachite green methoxide in polychlorostyrene (film type B).* Calibrations of the dosimeters were accomplished by ^{60}Co γ-ray irradiations. Previous studies have been made of their response characteristics when irradiated by photon and electron beams at various dose rates and under various environmental conditions. They are useful over a dose range of approximately 0.1 to 30 Mrad. It has been demonstrated further that the response is independent of (a) type of radiation (photons or electrons), (b) dose rate up to 10^{15} rad/s, and (c) energy spectrum (when greater than a few keV) [7-15]. For a given dose, the response of film type A varies with relative humidity but is the same in air, nitrogen, and vacuum; however, for a given dose, the response of film type B is insensitive to moisture but is different in air from that in oxygen-free environments. Both dosimeters show a variation of response with temperature during irradiation. In addition, they display a change in response if stored at elevated temperatures. For this study the films were calibrated, stored, and read at room temperature. Also, both types of dosimeters are sensitive to ultraviolet radiation, and hence must be protected from sunlight and white fluorescent lighting.

The energy deposition, or absorbed dose, in the dosimeters is interpreted from calibration curves by means of optical density transmission

*These dosimeters were obtained from Far West Technology,Inc., Goleta, California 93017. Film type A corresponds to the manufacturer's designation of FWT-60 and film type B to FWT-70. The identification of the commercial supplier is not intended as an endorsement but to specify more precisely the nature of the materials used.

measurements. At certain visible wavelengths, there are changes in the optical densities of the dye-film dosimeters due to irradiation. These changes are measured at or near the wavelengths of maximum optical density by means of a spectrophotometer or microdensitometer. The calibrations consist of a curve relating change in optical density at a given wavelength to absorbed dose in the film ("cavity") material. Cavity theory, employing appropriate stopping power relations between the medium and the cavity material, is applied to obtain the final desired results. This method lends itself to the measurement of high spatial-resolution distributions of absorbed dose since microdensitometer measurements can be made in a continuous fashion across the radiographic image produced in the film dosimeter.

In this study, homogeneous media of carbon, aluminum, polyethylene, and polystyrene have been irradiated with normally incident, 10-MeV electron beams to doses between 1 and 3 Mrad. The depth-dose distributions in these materials were derived from photometric readings of thin dye-film dosimeters placed at different depths inside these media. The radiation measurements were performed in a food processing facility using a scanned 10-MeV electron beam that is employed for irradiating food packages. Therefore, these data and conclusions are expected to be important in defining the relevant parameters in that application of radiation processing as well as in other areas such as sterilization of medical devices (sutures, surgical instruments, transplant apparatus), graft polymerization (textiles, ion-exchange membranes), polymer crosslinking (wire and cable insulators, heat-shrinkable tubing), and curing of coatings (inks, automobile parts, paint layers).

B. EXPERIMENTAL METHOD

B.1. Description of the Irradiation Facilities

Both types of dye-film dosimeters (A and B) were calibrated in the NBS ^{60}Co γ-ray pool source. Irradiations were also carried out in the Natick Laboratories ^{60}Co irradiators. Comparisons of these results are given in a later section of the report.

The NBS water-shielded ^{60}Co γ-ray source provides a dose rate of about 10^3 rad/s. It is made up of twelve encapsulated ^{60}Co pencils mounted upright in a 10.5-cm diameter circle on a baseplate at the bottom of a 3-meter deep water pool. The dye-film dosimeters were mounted in a polystyrene holder inside a watertight stainless-steel can during the calibration irradiations. The holder was sufficiently thick so as to provide electronic equilibrium conditions. The dosimeters were positioned in the center of the source. Figure 1 is a diagram of the arrangement of the sources, can, and film holder. During an irradiation, a constant flow of either dry nitrogen gas or dry air was maintained around the dosimeters. This procedure provided for calibration either in nitrogen or air and, at the same time, maintained a nearly constant ambient temperature of about 19°C.

At the Natick Laboratories, irradiations of the dye-film dosimeters were made in two different ^{60}Co γ-ray sources separately. One source provided a dose rate of about 40 rad/s and the other a rate of about 1.7×10^3 rad/s. Both sources are commercial, lead-shielded irradiators with automatic timing control of the exposure duration. The lower-activity source has an air-cooled irradiation chamber while the higher-activity source has an irradiation chamber in which the temperature

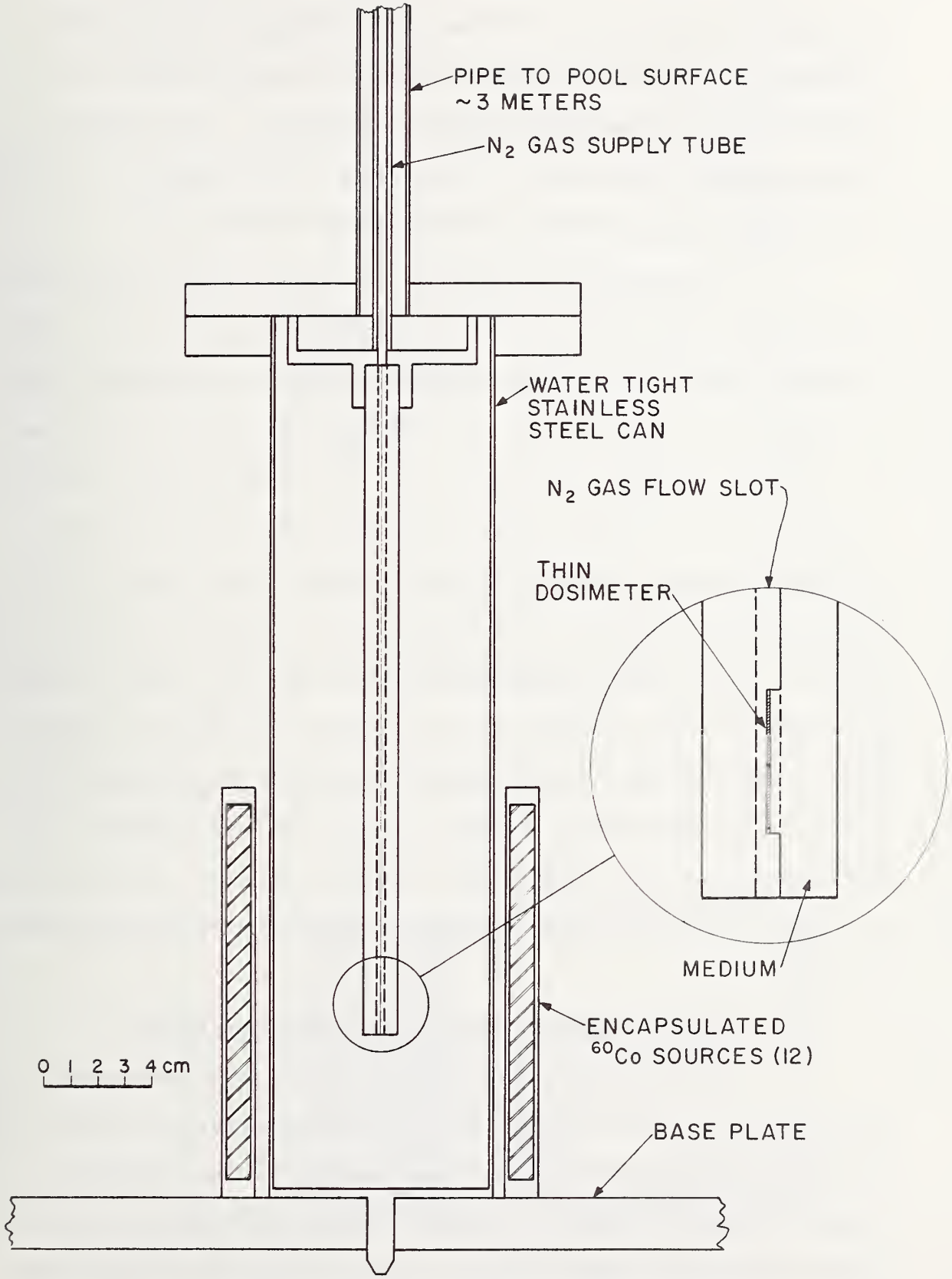

Figure 1. Schematic Diagram of the NBS ^{60}Co Pool Source, and Dye Film Holder.

is controlled by gas boiled off from liquid nitrogen. During irradiation, dosimeters were sandwiched between plates of polystyrene which are thick enough to provide electronic equilibrium conditions. These assemblies were positioned at the center of each source in the irradiation chambers, both of which were maintained at a temperature of about 25°C.

The electron source employed for the depth-dose measurements in the various materials was the Natick Food Laboratories' linac. Beam parameters under typical operating conditions for the irradiations were as follows: (a) energy of 10.0 ± 0.3 MeV, (b) pulse rate of 180 pulses per second, (c) pulse width from 2 to 5.5 μs, (d) peak current from 450 to 550 mA, and (e) average current from 200 to 500 μA. The beam was electromagnetically scanned in a vertical direction at a rate of 0.5 Hz. The beam passed through a 0.5-mm thick aluminum window of a scan horn into the air. At the sample irradiation position (about 20 cm from the aluminum window) the beam was about 3 cm in diameter and scanned a distance of about 40 cm in length. A servo-controlled conveyor moved material to be irradiated through the beam at right angles to the scan direction. For the conditions of these measurements, the peak dose rate was approximately 10^{10} rad/s. The average dose rate for a complete irradiation was about 10^{5} rad/s.

B.2. Material-Dosimeter Arrangements Under Irradiation

For the purpose of determining depth-dose distributions, thin dye-film dosimeters were incorporated in two arrangements in blocks of the various homogeneous materials that were irradiated. One arrangement is called the "wedge" method [16] which is illustrated in Figure 2, and the other is called the "stack" method. The square face of each block was

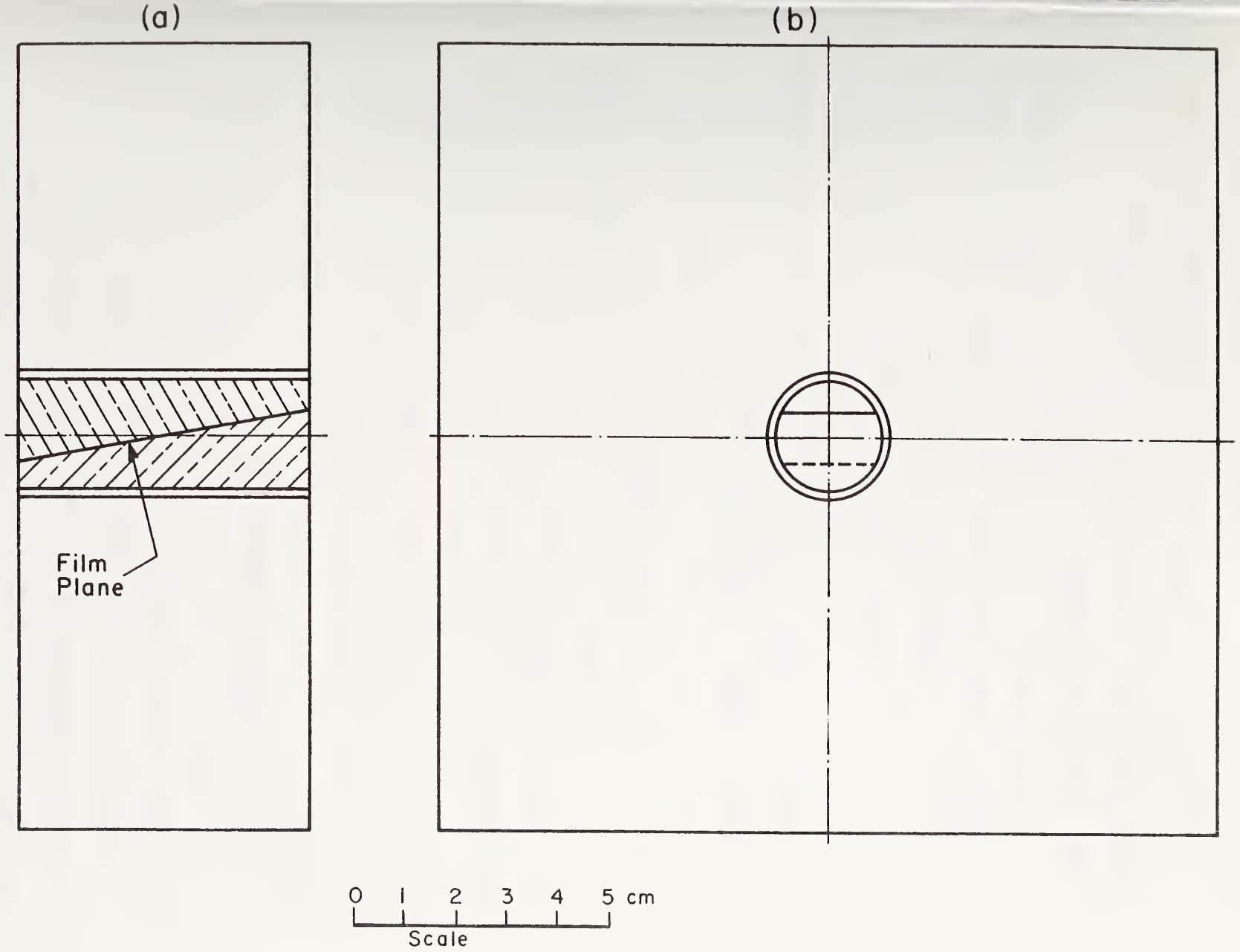

Figure 2. "Wedge" Method of Mounting Dye-Film Dosimeters in Homogeneous Medium; (a) Electron Beam Direction is Parallel to Page, (b) Electron Beam Direction is Perpendicular to Page.

perpendicular to the beam direction. Polyethylene and polystyrene had side dimensions of 15.2 cm and a thickness of 5.7 cm, carbon and aluminum had corresponding dimensions of 10.2 cm and 3.8 cm.

The two methods cited above were used to locate the dosimeters in the center of each block. These methods involve assemblies of homogeneous media and dosimeters which are described as follows: (a) The "wedge" is a solid cylinder which is slit lengthwise on a slant at an angle of about 9° to the beam direction. A strip of the dye-film dosimeter is placed in the slit. The two halves then are held tightly together with a hollow cylinder of 2.5-cm outside diameter, the cylinder being fitted into a hole in the center of the block. (b) The "stack" is a cylinder made up by alternately assembling disks of the block material and squares of the dosimeters. The disks are 2.2 cm in diameter and are 0.06 cm thick for carbon and aluminum and 0.30 cm thick for polyethylene and polystyrene. In the same manner as with the "wedge", a completed stack is held together with a hollow cylinder, and the entire assembly is located in the center of the block. During the irradiations, an additional piece of the dye-film was taped on the beam-entrance side of the assembly.

B.3. Optical Density Measurements

Before irradiation the two types of dye-film dosimeters are transparent and almost colorless. Upon irradiation, however, they become colored, and a plot of their optical densities versus optical wavelength shows broad characteristic absorption peaks in the visible region of the spectrum. Film type A develops a single broad asymmetric peak at about 601 nm (see Figure 3) while film type B exhibits two broad peaks, the

larger at 630 nm and the smaller at 430 nm (see Figure 4).

The absorbed dose received by the dosimeters is interpreted from a measurement of the change of optical density, ΔOD, at or near the absorption peaks produced by the radiation. These measurements are made with either a spectrophotometer or a microdensitometer equipped with interference filters. In the dose range between about 0.1 and 5 Mrad, the ΔOD is measured at 601 nm for film type A and at 630 nm for film type B. From 5 to 30 Mrad, the ΔOD is measured at 540 nm for type A and at 430 nm for type B; this procedure is necessary because above 5 Mrad the optical densities at 601 and 630 nm are beyond the accurate measurement range of the photometric instruments.

Spectrophotometer readings were made of optical density changes of the dye-film dosimeters used for the ^{60}Co calibrations and for those exposed in the "stack" method. Measurements of some, but not all, of these dosimeters were made both at NBS and at Natick Laboratories. The spectrophotometers at the two laboratories were cross-checked, and it was concluded that for a given dosimeter the readings were identical to within the precision of the optical density determinations.

Values of ΔOD at the appropriate absorption peak were determined by following a two-step procedure: (1) First an OD reading was taken at a wavelength far removed from the peaks, at 710 nm for film type A and at 780 nm for film type B. This base-line value was subtracted from the peak reading. This procedure corrected for the absorption, scattering, and reflection losses that were intrinsic for each individual dosimeter and that were not associated with the dye ion in the dosimeter. (2) The procedure just outlined was repeated for unirradiated control

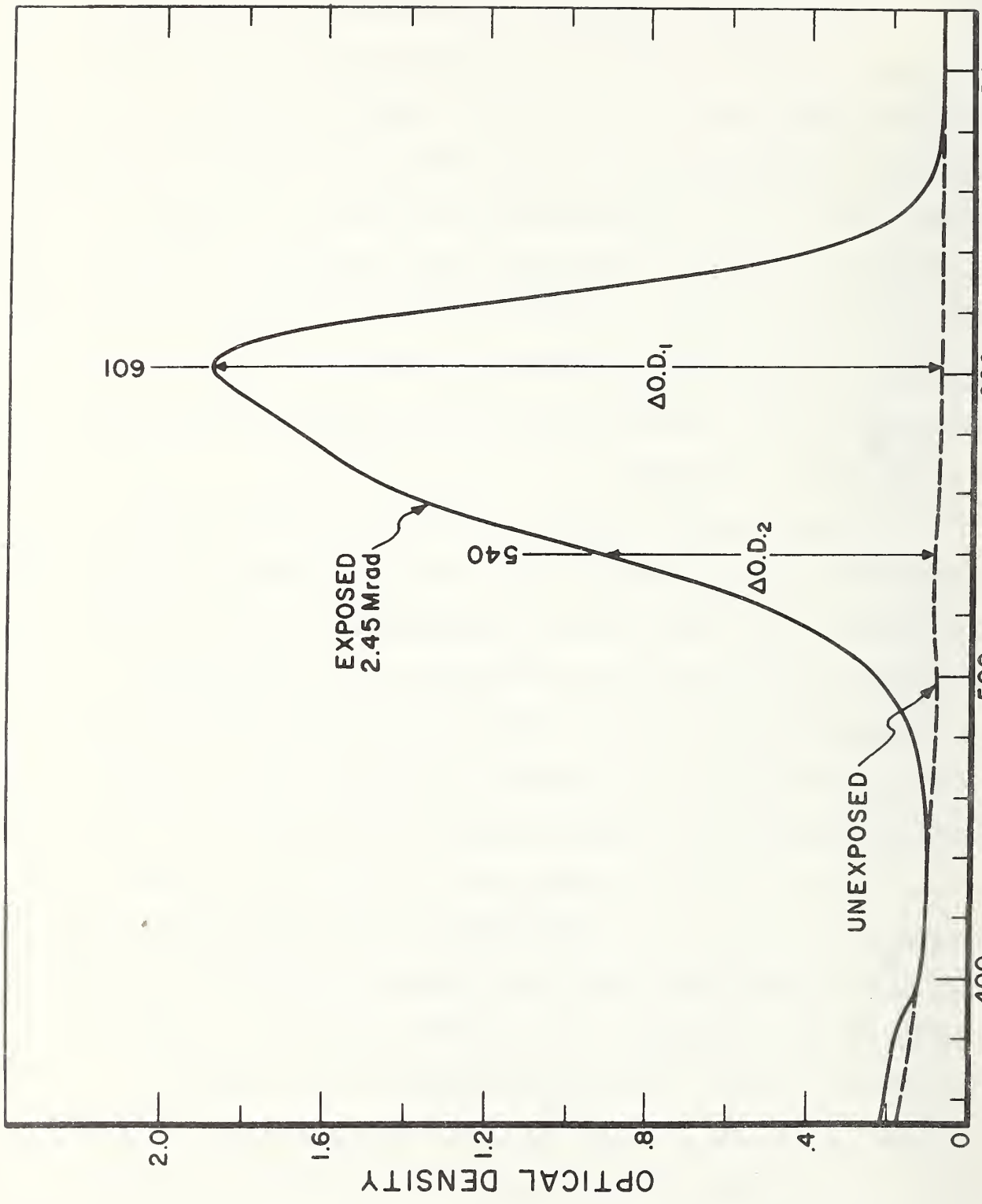

Figure 3. Optical Absorption Spectrum of Film Type A, Irradiated and Unirradiated.

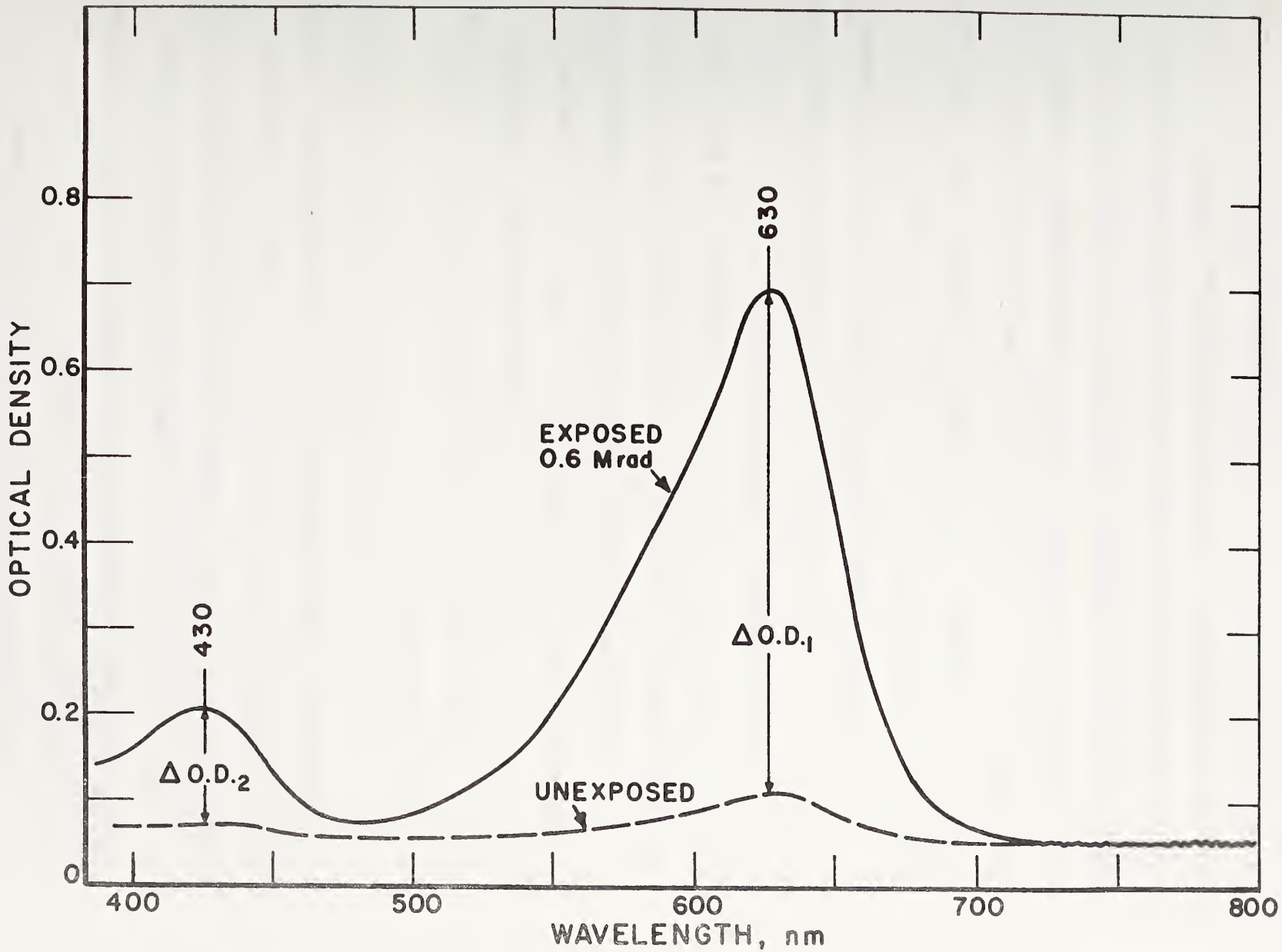

Figure 4. Optical Absorption Spectrum of Film Type B, Irradiated and Unirradiated.

films. (3) Then the ΔOD for a given dosimeter is equal to step (1) minus step (2) (see Figures 3 and 4). Care was taken to correct for an interference phenomenon that occurs with films of very uniform thicknesses and that results in oscillations of the optical density values over small changes in the wavelength [12,17]. The phenomenon is caused by interference of the light which has undergone multiple reflections at the air-dosimeter interfaces. In such cases, an average of the maxima and minima of the interference pattern is taken as the optical density.

Microdensitometer readings were made of the dye-film dosimeters irradiated in the "wedge" method. The optical density measurements were taken with this instrument using narrow band-pass, Fabry-Perot interference filters which were centered on wavelengths of 600 nm for film type A and 430 nm for film type B. A cross check was made of the response of the microdensitometer and the spectrophotometer. To accomplish this, readings were taken on 35 dosimeters of film type A and 22 dosimeters of film type B. The average ΔOD from the spectrophotometer readings was about 1.6 percent higher than that of the microdensitometer readings for both types of dosimeters.

In order to account for the effect of variations in thickness for individual dye-film dosimeters, ΔOD for each dosimeter was divided by its thickness in millimeters so that the variable followed with absorbed dose is the change in optical density per unit thickness in units of ΔOD/mm. A dial-indicating micrometer with an accuracy of ±1% was used to measure the thickness of each dosimeter. The nominal thickness of the dye-films was of the order of 50 μm.

Two different batches of film type B were employed. They are

designated as film types B-1 and B-2. Film type B-1 was obtained from the supplier about 2 years ago as sheets with dimensions of 20 by 25 cm, whereas film type B-2 was obtained about a month before irradiation and was in the form of 1 by 1 cm squares. The two batches showed slightly different responses to radiation.

C. RESULTS

C.1. Calibration of the Dosimeters

The dye-film dosimeters were calibrated in the NBS ^{60}Co γ-ray pool source. The output of this source has been determined previously to a high accuracy with the use of a carbon (graphite) calorimeter and a cavity ionization chamber [18]. Results of the dosimeter calibrations are shown in Figure 5 for film type A and in Figure 6 for film type B.

During the calibration irradiations, the dosimeters were embedded in a cavity within the polystyrene holder. The thickness of material surrounding the dosimeters was such that it provided electronic equilibrium in the cavity, that is, the material thickness was equal to the range of the most energetic secondary electron that could be generated by photons in the polystyrene holder. From the original calibration, the ^{60}Co γ-ray source output had been determined as the dose rate in carbon. For any other material, the absorbed dose is given by the following formula [19]:

$$D_m = D_c \frac{\left(\frac{\bar{\mu}_{en}}{\rho}\right)_m}{\left(\frac{\bar{\mu}_{en}}{\rho}\right)_c} = D_c \left(\frac{\bar{\mu}_{en}}{\rho}\right)_{m/c} \qquad (1)$$

where the subscripts m and c indicate the material and carbon respectively; D is the absorbed dose; and $\frac{\bar{\mu}_{en}}{\rho}$ is the mass energy absorption coefficient averaged over a given energy range. Equation (1) can also be applied to determine the dose rate by substituting $\dot{D}$ for D. For these results, the ratio of the average mass energy absorption coefficients

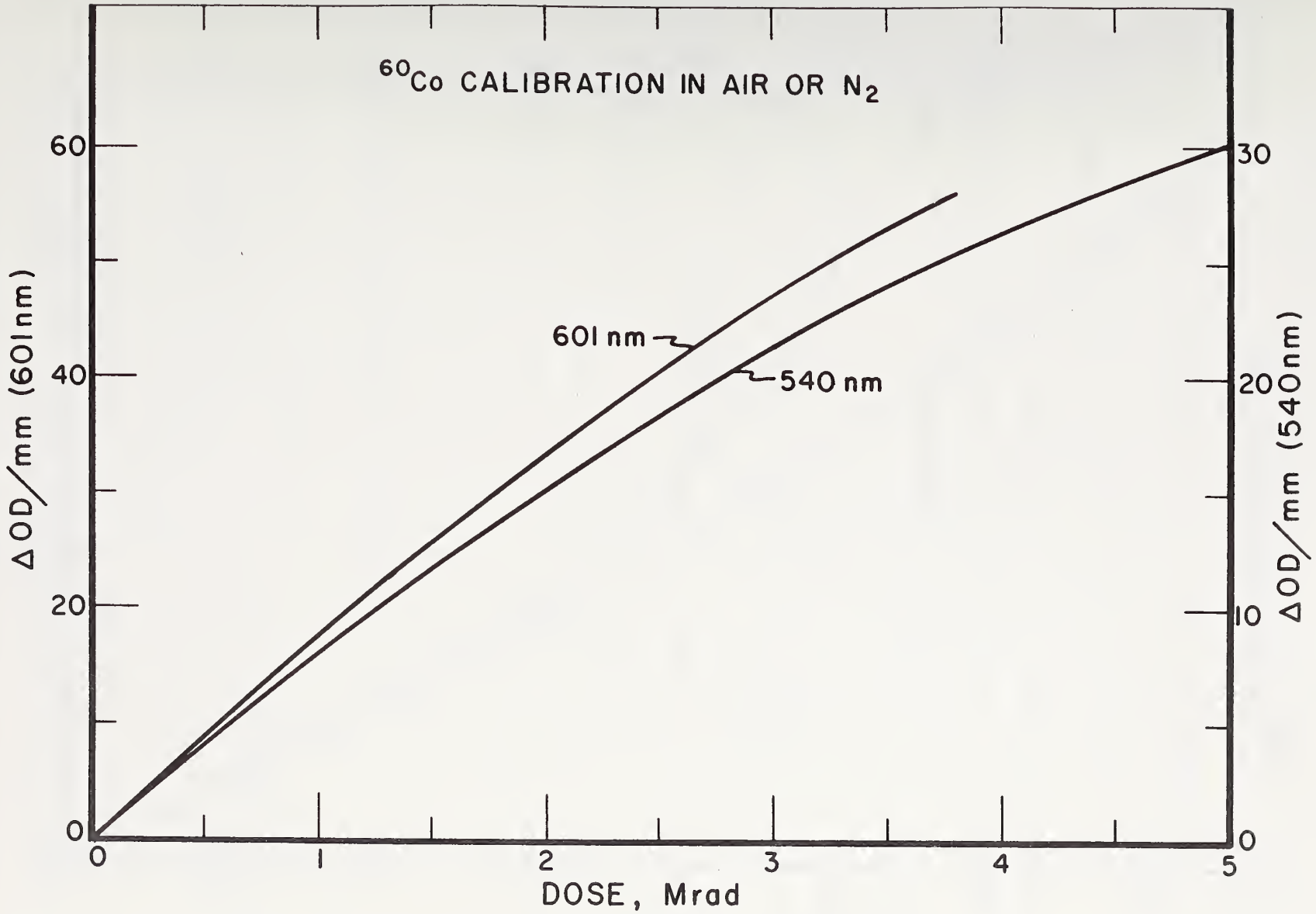

Figure 5. ^{60}Co γ-ray Calibration Curves of Film Type A in Air or Nitrogen Atmosphere. Optical Densities Measured at Two Wavelengths.

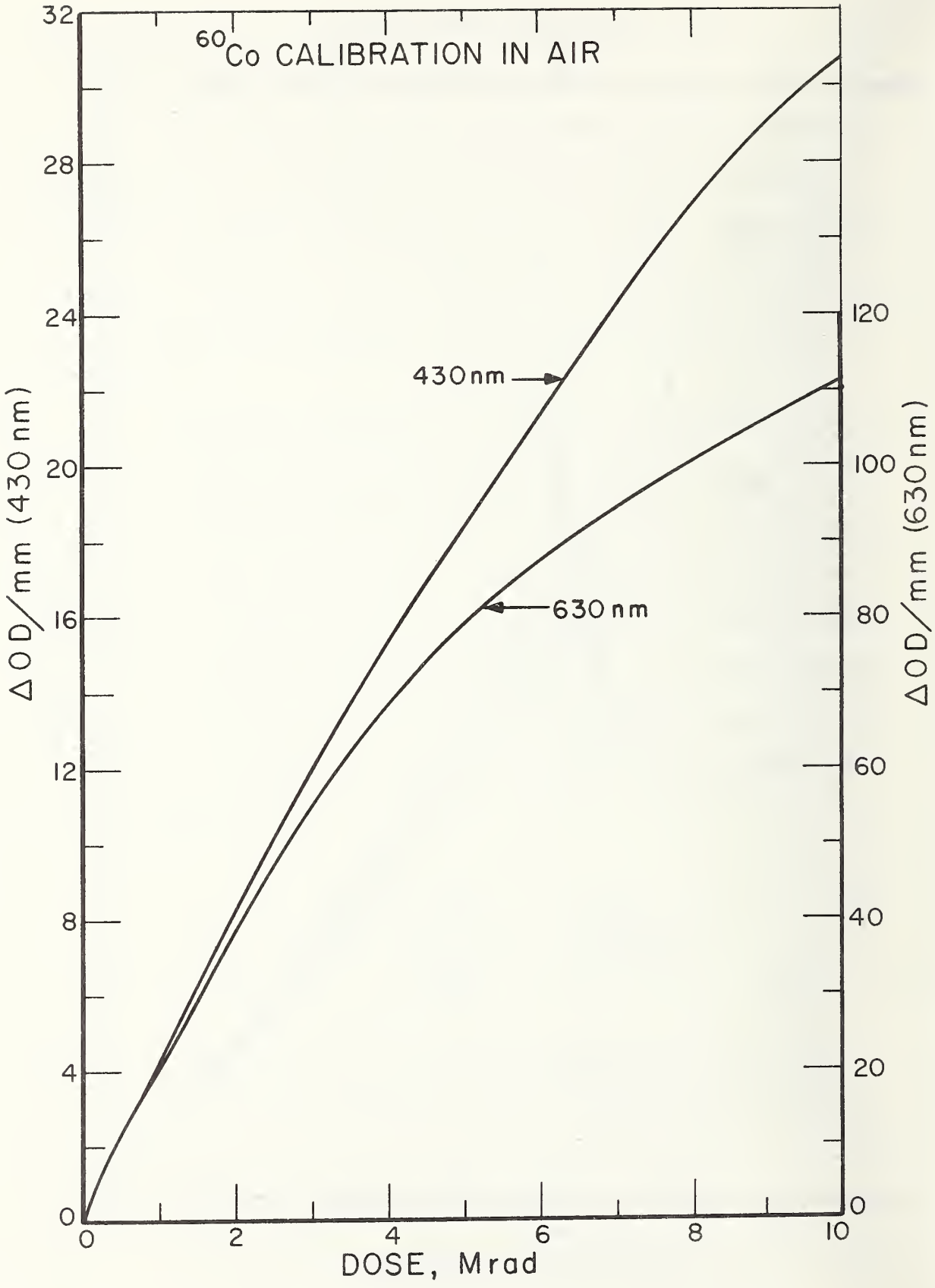

Figure 6. ^{60}Co γ-ray Calibration Curves of Film Type B in Air. Optical Densities Measured at Two Wavelengths.

(of polystyrene to carbon) was taken to be equal to 1.077. This value was within ±0.3 percent of all such ratios that exist over the range of photon energies from 0.1 to 1.3 MeV. Ratios were computed from tabulated values of the mass energy absorption coefficients as a function of photon energy [20].

In order to determine the absorbed dose in the dosimeters irradiated in a medium, cavity theory was applied [1, 21, 22]. This theory is applicable if the following conditions are met:

a. The cavity containing the dosimeter is small or thin with respect to the range of most secondary electrons, that is, the number of secondary electrons produced in the dosimeter must be negligible compared to the number produced in the surrounding material;

b. The electron energy spectrum at any depth must be essentially undisturbed by the presence of the cavity; and

c. The photon and electron fluence as well as energy-loss profiles must be spatially uniform and continuous close to the cavity. These conditions were met in all cases for the results described in this study. Hence, if D_m is the absorbed dose in the medium, then, D_f, the absorbed dose in the dye-film dosimeter is

$$D_f = \bar{s}_{f/m} \cdot D_m \quad , \tag{2}$$

where $\bar{s}_{f/m}$ is the ratio of the electron mass collision stopping powers of the dosimeter to the material averaged over a given energy range. Electron mass collision stopping powers have been calculated for a number of materials and these values have been tabulated as a function of electron energy [23, 24]. For the dye-film dosimeter in a polystyrene holder,

the following average values of the mass collision stopping power ratios of the film to polystyrene were used: (a) film type A = 1.031 and (b) film type B = 0.948. These average ratio values were within ±0.5 percent of all such ratios over the energy range from 0.1 to 1.3 MeV.

The results shown in Figures 5 and 6 were obtained by combining Equations (1) and (2); that is, in general

$$D_f = D_c \cdot \left(\frac{\bar{\mu}_{en}}{\rho}\right)_{m/c} \cdot \bar{s}_{f/m} \quad . \tag{3}$$

In this way, the measured dosimeter response of the change in optical density was related to the absorbed dose in the dosimeter.

C.2. A Comparison of Dose Rates of the NBS and the Natick Laboratories ^{60}Co γ-ray Sources

The output of the ^{60}Co γ-ray irradiators at the Natick Laboratories had been determined with the Fricke (ferrous sulfate) dosimeter, which is primarily an aqueous system. Therefore, the dose rate specified was that in water. The equation used to find the dose in the dye-film dosimeters was the following:

$$D_f = D_w \cdot \left(\frac{\bar{\mu}_{en}}{\rho}\right)_{m/w} \cdot \bar{s}_{f/m} \tag{4}$$

where w refers to water, and m refers to the material (polystyrene) of which the film holders were made. The value of $\left(\frac{\bar{\mu}_{en}}{\rho}\right)_{m/w}$ is 0.965 which is within ±4 percent of the ratio values computed for polystyrene to water between 0.1 and 1.3 MeV.

Table 1 gives a comparison of the NBS and the Natick Laboratories (one air-cooled and another nitrogen-cooled) ^{60}Co sources on the basis of total absorbed dose in the dye-film dosimeters. Within the limits of error, the ratio of the responses of film type A indicates the

Table 1

Comparison of Dose Rates of the NBS and Natick Laboratories ^{60}Co γ-ray Sources†

A. Film Type A

Ratio of Dose Readings: NBS/Natick Laboratories

Air	0.955 ± 0.048
N_2	0.980 ± 0.029

B. Film Type B

Ratio of Dose Readings: NBS/Natick Laboratories

	Film Type B-1		Film Type B-2	
	430 nm	630 nm	430 nm	630 nm
Air(a)*	0.937±0.037	0.892±0.018	0.996±0.030	1.054±0.063
Air(b)	0.939±0.056	0.992±0.040	0.984±0.010	1.039±0.010
N_2(a)	0.823±0.016	0.837±0.008	0.930±0.056	1.013±0.030
N_2(b)	0.842±0.034	0.848±0.008	0.938±0.019	1.024±0.010
$\overline{\text{Air}}$	0.940 ± 0.080		1.018 ± 0.070	
$\overline{N_2}$	0.838 ± 0.039		0.976 ± 0.069	

Note: †The approximate dose rates in the dosimeters at the time of exposure were: 710 rad/s at NBS, 42 rad/s in air and 1700 rad/s in N_2 at Natick Laboratories.

*Air(a) and N_2(a) data are for spectrophotometric readings 1 to 2 days after irradiation. Air(b) and N_2(b) data are for readings 7 months after irradiation. $\overline{\text{Air}}$ and $\overline{N_2}$ data are average values.

outputs of the Natick Laboratories sources are as specified by their previous calibrations. The same conclusions can be made for film type B-1 in the air-cooled source and film type B-2 in both sources; however, film type B-1 does indicate a significant difference for the nitrogen-cooled source. The values of the ratios of the two sources were calculated by averaging all values for the individual measurements as indicated in Table 1. An associated error was assigned which is equal to the square root of the sum of the squares of the errors assigned to the individual measurements.

A difference was found between the two types of films (A and B) in their post-irradiation coloration development. Film type A showed a 2 to 3 percent increase in optical density during the first two days following irradiation, but thereafter was stable. A gradual increase could be seen in the optical density of film type B for several weeks following irradiation; therefore, the time between an irradiation and a photometric reading had to be monitored so that a proper correction factor could be applied when comparing dosimeters read at different times. Since some of film type B-1 were read after an elapsed time of 7 months, post-irradiation development seems not to be the cause of the results in the nitrogen-cooled source. A satisfactory explanation of these anomalous results of the film type B-1 measurements has not been proposed to date.

C.3. Depth-Dose Distributions in Electron Irradiated Materials

The four homogeneous materials irradiated by incident 10-MeV electrons were carbon, aluminum, polyethylene, and polystyrene. The dose versus depth curves for these materials as measured with film type

A are shown in Figures 7 and 8, where T_o is the incident electron energy and R_e is the extrapolated (practical) range. Nominal entrance doses in water were 1.0 Mrad for carbon and aluminum and 1.5 Mrad for polyethylene and polystyrene. The discrepancy observed in Figure 8 between stack and wedge data in polystyrene will be discussed in a later section. The depth-dose distributions as measured with film type B are shown in Figure 9 through 12, where ρ is the material (medium) density and T_o is the incident electron energy. Film type B-1 was used in the "wedge" method measurements and film type B-2 was used in the "stack" method measurements. For these measurements, the nominal entrance dose in water was 2.0 Mrad for all materials. The doses in the homogeneous materials were interpreted by measuring the ΔOD in film type B at both 430 and 630 nm for the "stack" method. A difference in values at the two wavelengths is noticeable for carbon (see Figure 9). This was apparently caused by damage that occurred to the surfaces of the dosimeters and resulted in less light transmission. Therefore, the curves were based entirely on the 630 nm measurements since the response at this wavelength is about four times greater than the response at 430 nm and is therefore less sensitive to this surface effect.

The absorbed dose in the material was determined by the use of Equation (2) which can be rewritten as

$$D_m = \bar{s}_{m/f} \cdot D_f \quad . \tag{5}$$

The values of the stopping power ratios used in these determinations are given in Table 2. These values were weighted averages over the energy range from 0.5 to 10.0 MeV. The percent variations over that energy range also are seen to be small, especially for film type B.

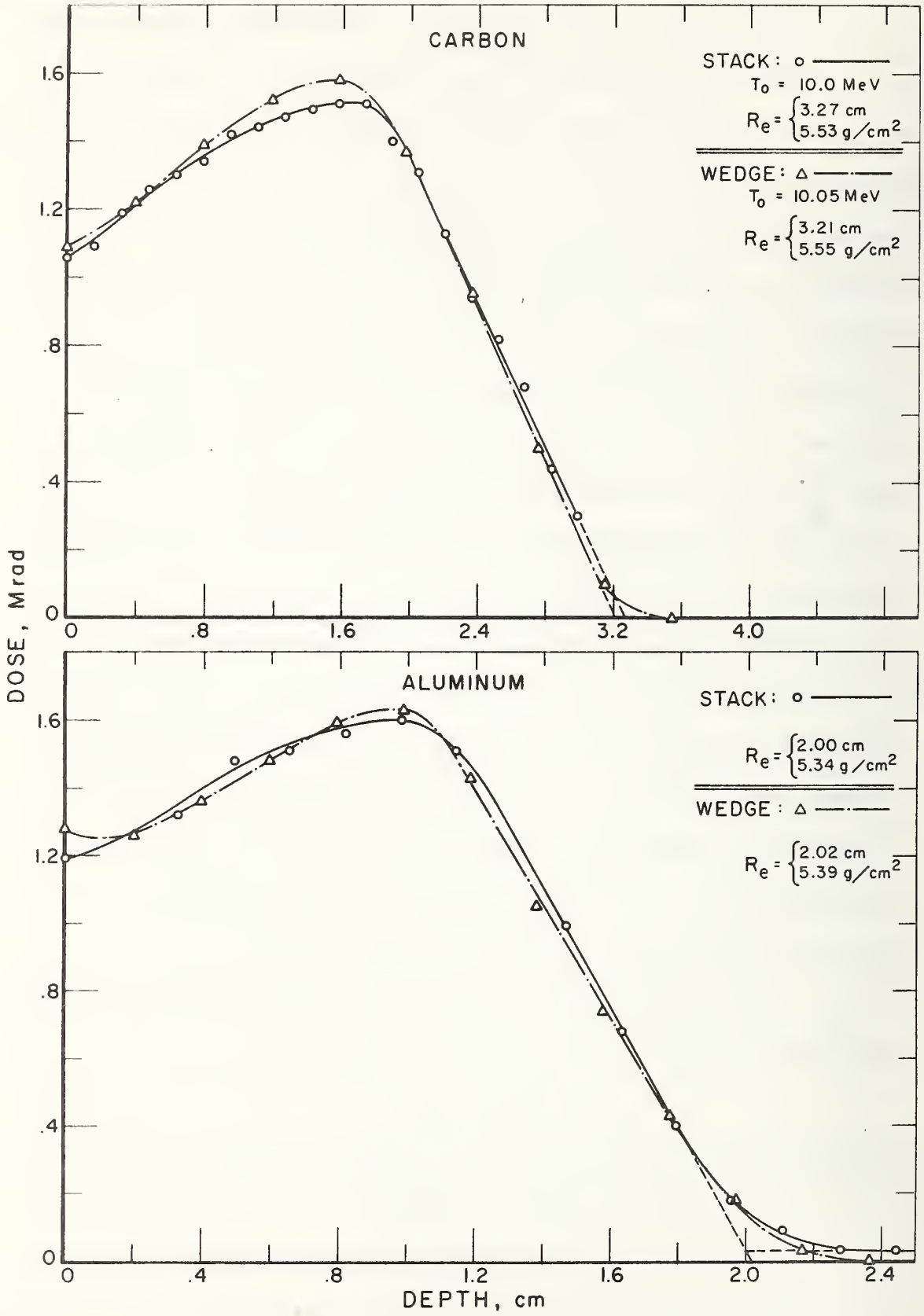

Figure 7. 10-MeV Electron Depth-dose Distributions in Carbon and Aluminum Measured With Film Type A

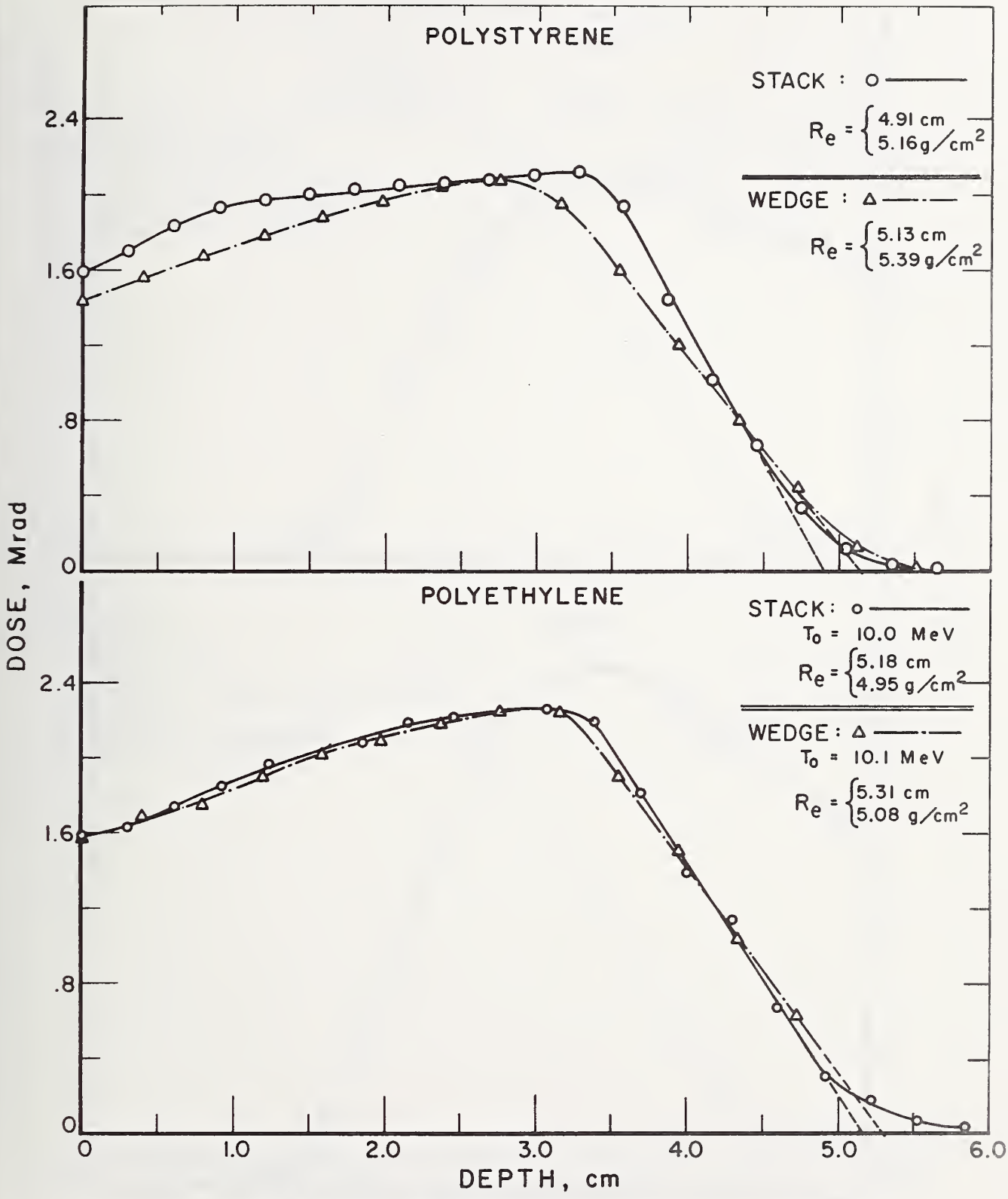

Figure 8. 10-MeV Electron Depth-Dose Distributions in Polystyrene and Polyethylene Measured With Film Type A.

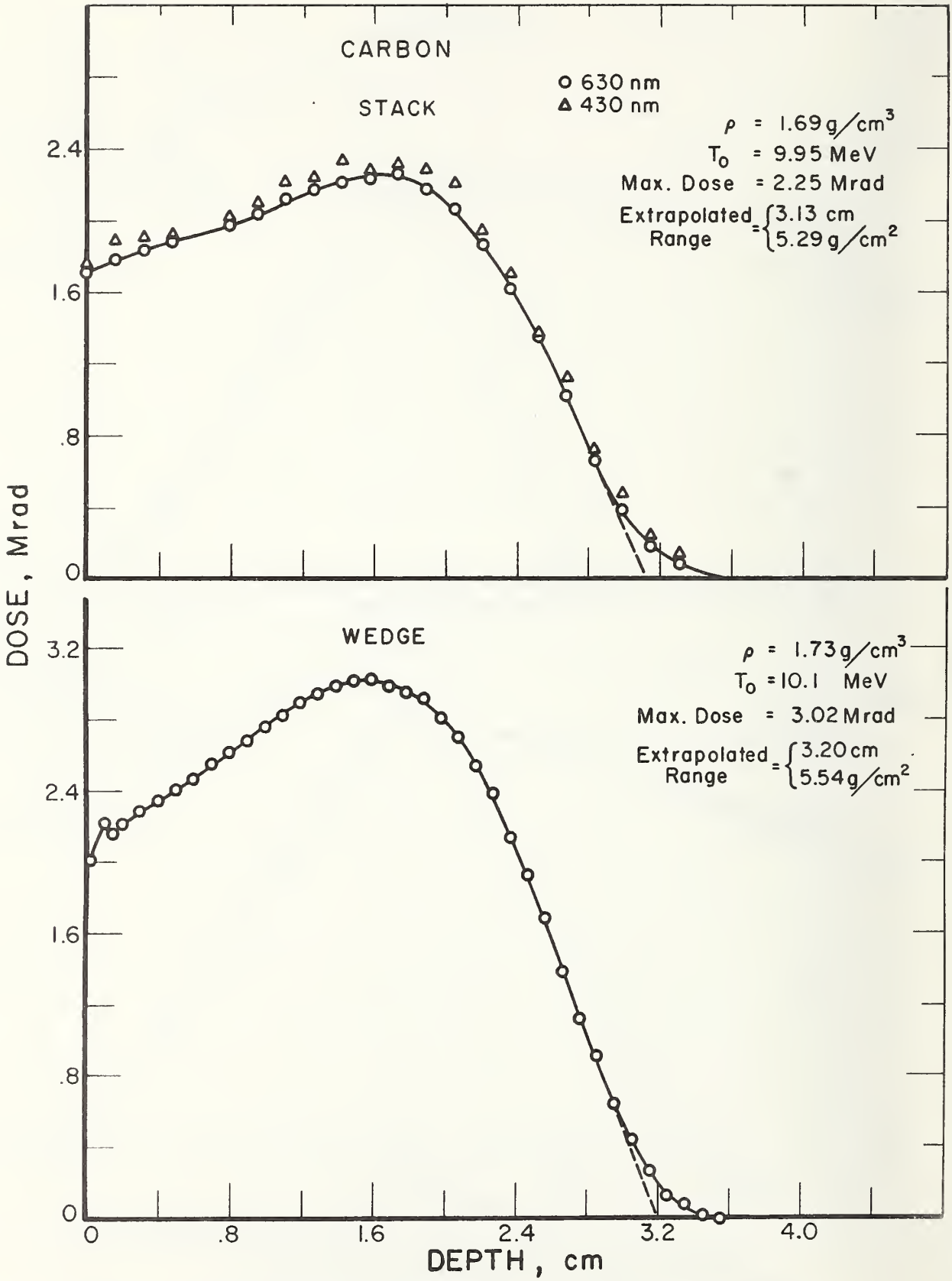

Figure 9. 10-MeV Electron Depth-Dose Distributions in Carbon Measured With Film Type B.

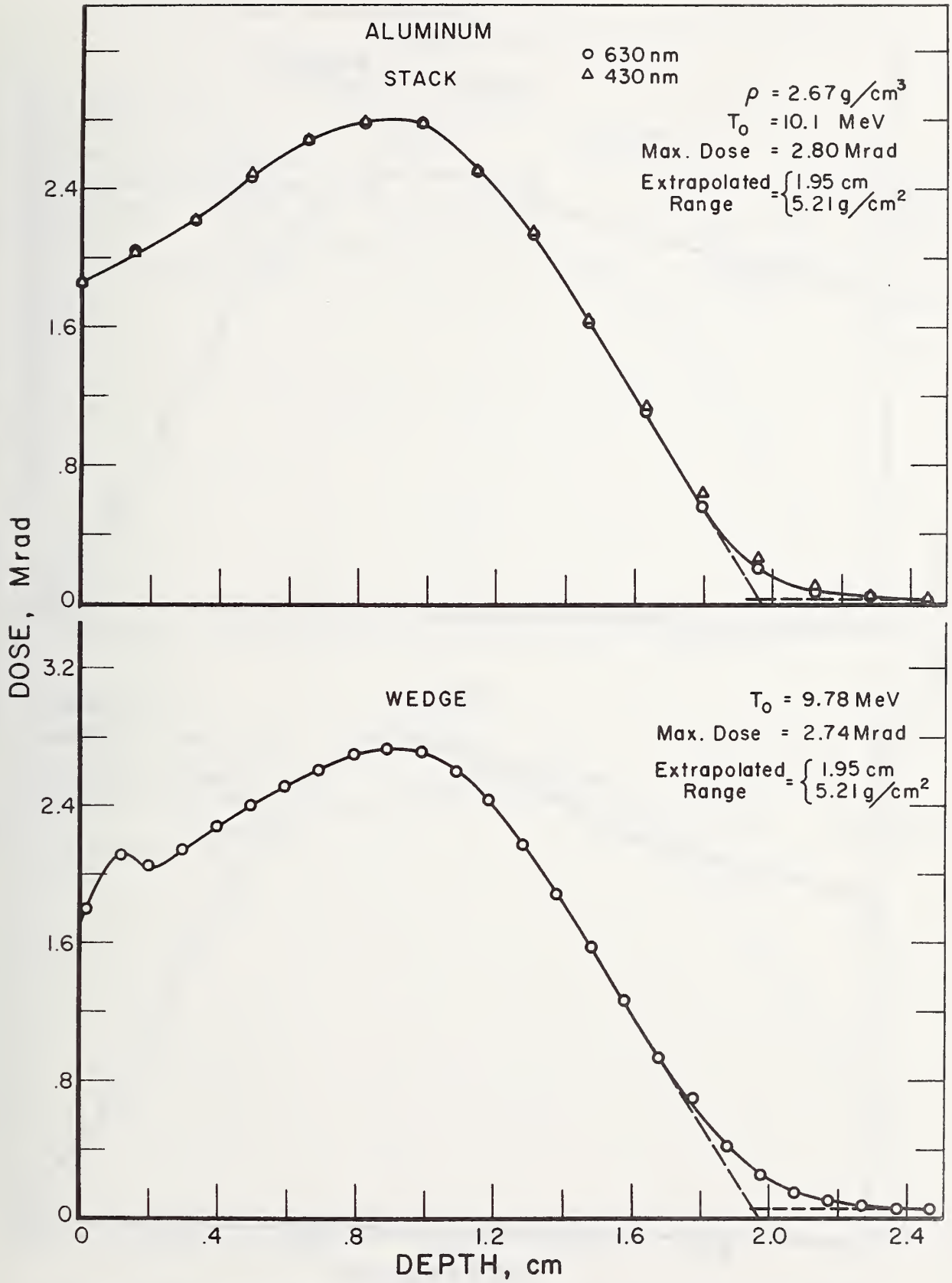

Figure 10. 10-MeV Electron Depth-Dose Distributions in Aluminum Measured With Film Type B.

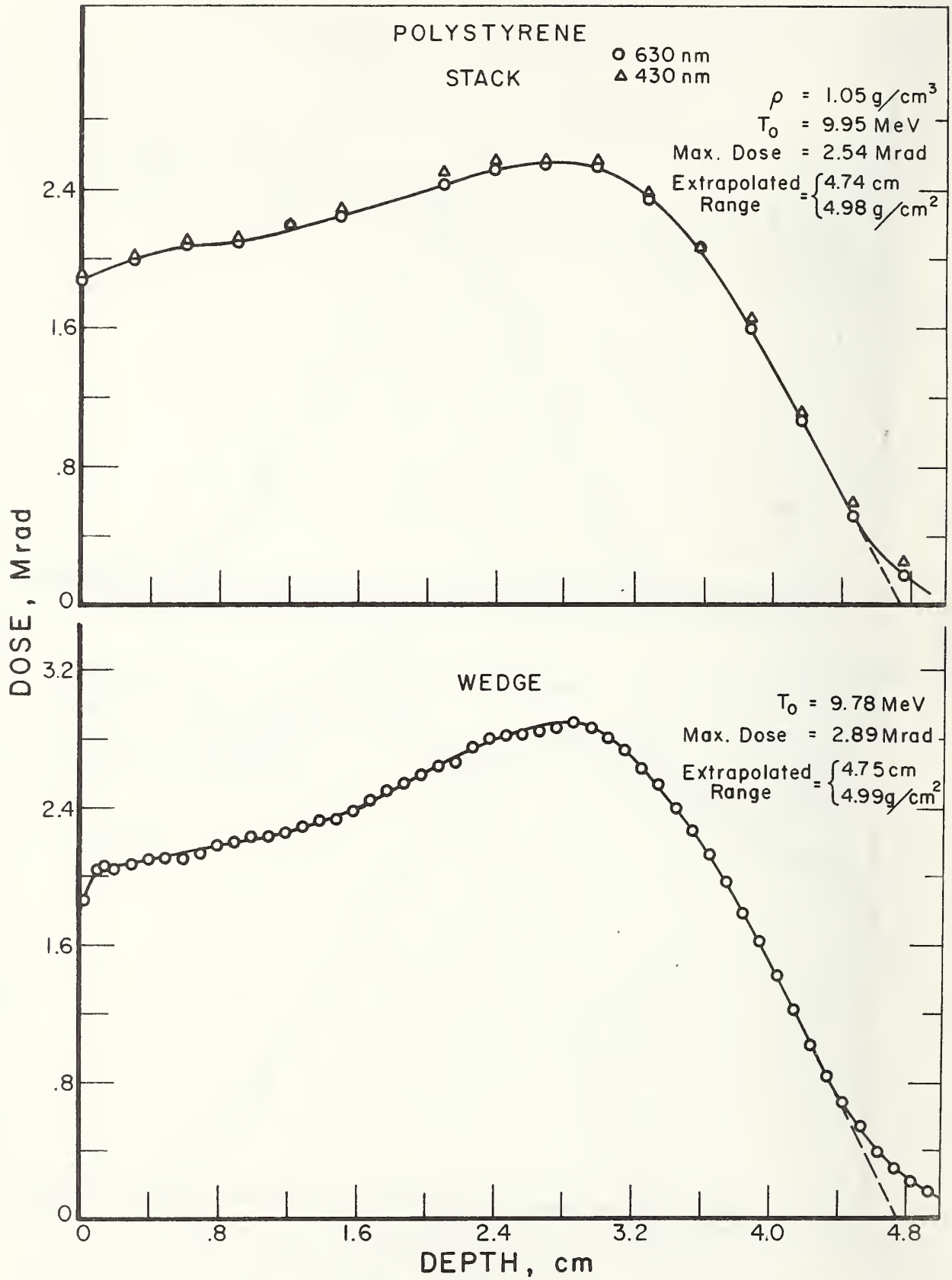

Figure 11. 10-MeV Electron Depth-Dose Distributions in Polystyrene Measured With Film Type B.

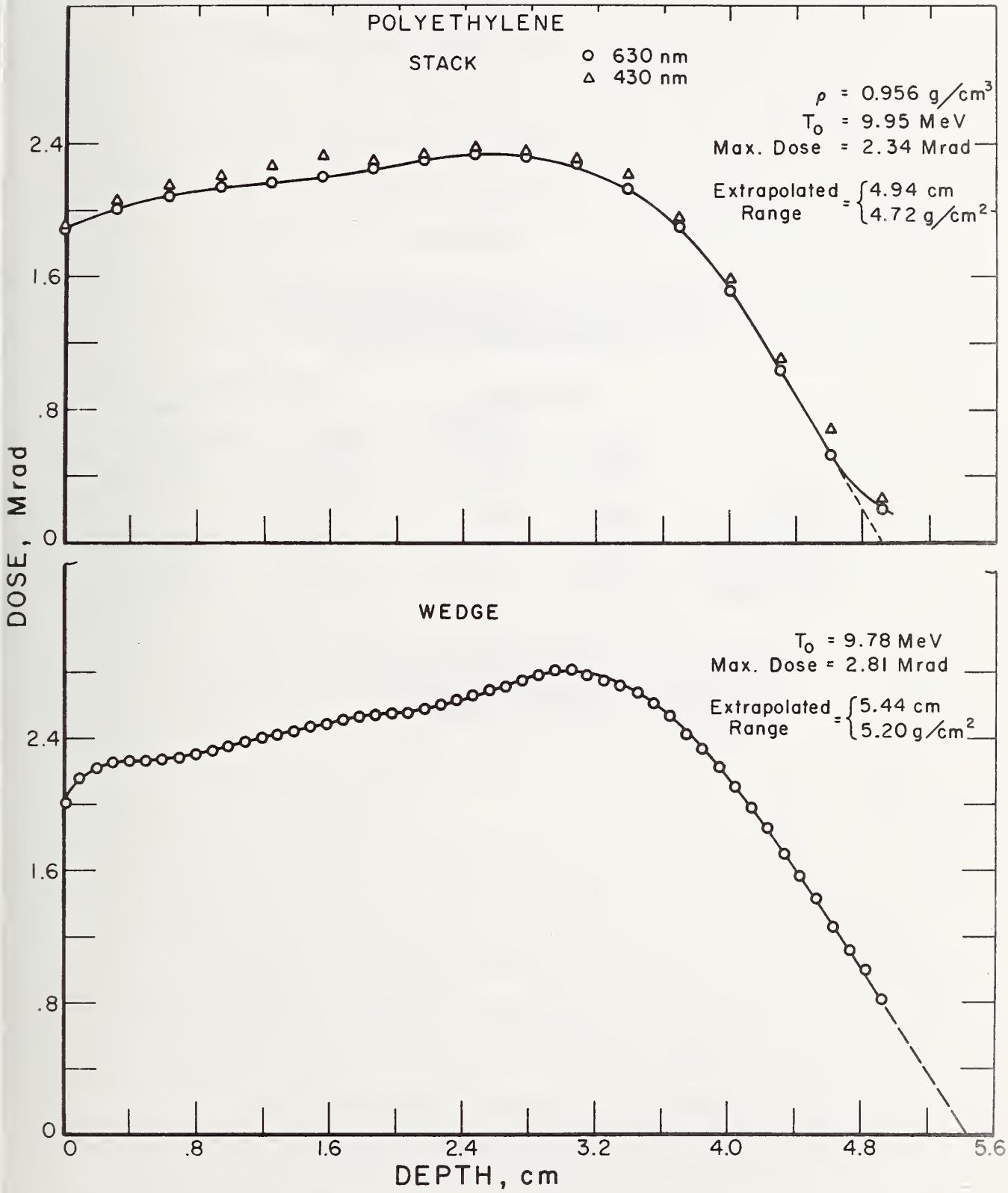

Figure 12. 10-MeV Electron Depth-Dose Distributions in Polyethylene Measured With Film Type B.

Table 2

Electron Mass Collision Stopping Power Ratios, Material to Film†

	Film Type A		Film Type B	
	Ratio	Percent* Variation	Ratio	Percent* Variation
Carbon	0.863	±1.6	0.947	±0.6
Aluminum	0.816	±5.0	0.873	±1.7
Polyethylene	1.016	±3.0	1.109	±1.6
Polystyrene	0.951	±2.3	1.041	±1.6

†Values in the table are from reference [24].

*The percent variation is over the electron energy range between 0.5 and 10 MeV.

Comparisons of experimental and calculated 10-MeV electron depth-dose distributions in carbon and aluminum are shown in Figure 13. The experimental curves were derived from the "stack" measurements using film type B (see Figures 9 and 10) while the histograms were obtained from Monte Carlo calculations of Berger and Seltzer [23]. The calculated results have been normalized to the experimental incident electron fluence in each case. No comparable comparisons are shown for polyethylene or polystyrene because calculated results are not available for those materials.

Table 3 gives some of the important parameters by which the depth-dose distributions can be characterized. The parameters listed are: (a) the depth of maximum dose, X_p, which occurs at the peak of the distribution, (b) the experimental extrapolated range, R_e, which is obtained by a linear graphical extrapolation to zero dose (or background) of the depth-dose curve beyond the depth of maximum dose, (c) the calculated extrapolated range, R_e', which is obtained in the same manner as R_e from the calculated depth-dose curves shown in Figure 13, and (d) the average electron pathlength, R_o, as determined by the continuous-slowing-down-approximation [24, 25]. The experimental values listed are averages obtained from data provided by the "stack" and "wedge" method measurements. A comparison of the parameters as determined by the two different dosimeters indicate agreement to better than 2 percent for carbon, 7 percent for aluminum, and 8 percent for both polyethylene and polystyrene.

The extrapolated (or practical) range in aluminum can be calculated from the following formula derived by Katz and Penfold [26]:

$$R_c = 0.530\ E_o - 0.106 \qquad (6)$$

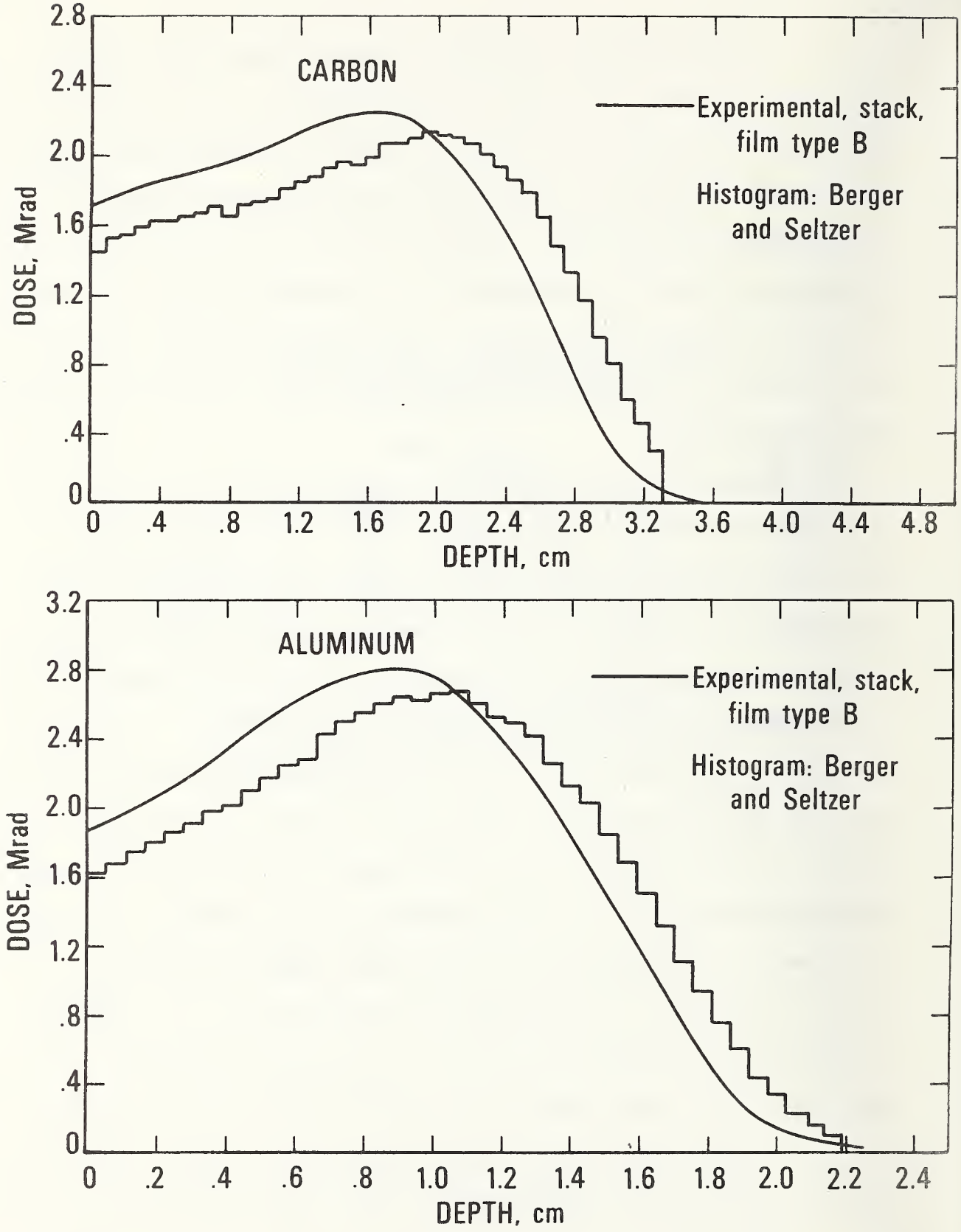

Figure 13. Experimental and Calculated 10-MeV Electron Depth-Dose Distributions in Carbon and Aluminum.

Table 3

Comparison of Some Experimental and Calculated Depth-Dose Parameters for the Different Materials†

	X_p (g/cm²)	R_e (g/cm²)	R'_e (g/cm²)	R_o (g/cm²)	R_e/R'_e	R_e/R_o
Carbon (A)*	2.68	5.54	5.75	5.58	0.963	0.993
Carbon (B)	2.74	5.42	5.75	5.58	0.943	0.971
Aluminum (A)	2.58	5.36	5.54	5.84	0.968	0.918
Aluminum (B)	2.42	5.21	5.54	5.84	0.940	0.892
Polyethylene (A)	2.84	5.02		4.79		1.048
Polyethylene (B)	2.63	4.96		4.79		1.035
Polystyrene (A)	3.11	5.28		5.10		1.035
Polystyrene (B)	2.88	4.98		5.10		0.976

Note: †X_p = depth of maximum dose, i.e., the peak of the depth-dose distribution.

R_e = experimental extrapolated range obtained by graphical extrapolation to zero dose of the depth-dose distribution.

R'_e = calculated extrapolated range obtained in same manner as R_e from reference [23].

R_o = mean electron pathlength from reference [24].

* The letter enclosed in parenthesis is the film type.

where R_c is the extrapolated (practical) range in g/cm^2 and E_o is the incident electron energy in MeV. This formula gives a value of $R_c = 5.19$ g/cm^2 for 10.0 MeV (average electron beam energy for irradiations of aluminum with film type A), and $R_c = 5.16$ g/cm^2 for 9.94 MeV (average beam energy for irradiations with film type B). The experimental extrapolated ranges for the two different dosimeters in Table 3 are in general agreement with these calculated practical ranges in aluminum. The ratio of the values are: $R_e/R_c = 1.033$ for film type A, and $R_e/R_c = 1.010$ for film type B.

Table 4 shows a comparison of the peak and entrance doses in the various materials as determined by the two dosimeters and by the two different methods of measurements. Generally, the ratio of the peak to entrance dose, D_p/D_e, from the two different methods ("stack" or "wedge") agree to better than 10 percent for a given material and dosimeter. If an overall average is taken, the ratio D_p/D_e for film type A is 1.41, and for film type B is 1.40. Therefore, within ±10 percent (+10 percent for aluminum and -10 percent for polyethylene, both for film type B), the ratio of D_p/D_e can be taken to be 1.40 for all materials.

The results obtained by the "stack" and "wedge" methods are compared in Table 5. Ratios are given of the "stack" to "wedge" methods for the peak dose, D_p; depth at the peak dose, X_p; and the extrapolated range, R_e. Perhaps the most sensitive parameter for comparison is X_p, the depth at the peak dose. That parameter agrees to within 5 percent for all materials except for polyethylene, as measured with film type B (see Figure 12), and polystyrene, as measured with film type A (see

Table 4

Peak and Entrance Doses of Depth-Dose Distributions

Film Type A

	Stack-S Wedge-W	D_e(Mrad)	D_p(Mrad)	D_p/D_e*
	S	1.06	1.51	1.42
Carbon	W	1.06	1.58	1.49
	S	1.19	1.60	1.34
Aluminum	W	1.18	1.63	1.38
	S	1.58	2.26	1.43
Polyethylene	W	1.57	2.26	1.44
	S	1.59	2.12	1.33
Polystyrene	W	1.43	2.07	1.45

Film Type B

	S	1.71	2.25	1.32
Carbon	W	2.08	3.02	1.45
	S	1.86	2.80	1.51
Aluminum	W	1.74	2.74	1.57
	S	1.89	2.34	1.24
Polyethylene	W	2.17	2.81	1.29
	S	1.88	2.54	1.35
Polystyrene	W	2.00	2.89	1.44

*Symbols D_e and D_p represent entrance dose and peak dose, respectively, in the material specified.

Table 5

Comparison of Results of the "Stack" and "Wedge" Methods of Depth-Dose Measurements

	Ratio of Response: "Stack"/"Wedge"[+]		
	D_p	X_p	R_e
Carbon (A)[*]	0.956	1.050	0.996
Carbon (B)	0.745	1.026	0.955
Aluminum (A)	0.982	0.969	0.991
Aluminum (B)	1.022	0.988	1.000
Polyethylene (A)	1.000	1.025	0.974
Polyethylene (B)	0.833	0.833	0.908
Polystyrene (A)	1.024	1.214	0.957
Polystyrene (B)	0.879	0.986	0.998

Note: [+]The symbols are: D_p = peak dose; X_p = depth at peak dose; and R_e = extrapolated, experimental range.

[*]The letter in parenthesis indicates the film type.

Figure 8). A close inspection of the curves indicate that the "wedge" data for polyethylene with film type B and the "stack" data for polystyrene with film type A appear to be inconsistent with other data. Probable causes for these results could have been (a) that in the "wedge" the material was not forced together sufficiently tight so that a gap existed between the material and the type B dosimeter and (b) that in the "stack" the irradiated polystyrene block discharged during or shortly after exposure, the light from which could have caused additional coloration of the type A dosimeters. However, overall the data indicate that there is no significant difference in the results obtained by these two methods.

D. CONCLUSIONS

D.1. Comparison of Experimental Results With Theory

This study has demonstrated that thin dye-film dosimeters can be employed successfully to determine depth-dose distributions in materials. First of all, the extrapolated ranges measured experimentally in aluminum are in excellent agreement with the range calculated by the Katz and Penfold formula [26]. The experimental ranges are also in reasonably good agreement with the theoretical mean pathlength ranges of Berger and Saltzer [24] as shown in Table 3. For 10-MeV electrons the calculated pathlengths are expected to be fairly close to the experimental ranges for low Z (atomic number) materials and become progressively larger than the experimental ranges with increasing Z. The ratios of R_e/R_o in Table 3 appear to confirm this premise. Other favorable comparisons are shown in Table 6 where Monte Carlo calculated [23] and experimental depth-dose distribution parameters for carbon and aluminum are compared. There is good agreement except for the depth of the peak dose in carbon and for the peak-to-entrance dose ratio in aluminum. Detailed comparisons of the carbon and aluminum experimental data with the calculations are shown in Figure 13. The measured depth-dose distributions are shifted toward the beam-entrance surfaces of the media relative to the calculated distributions. One possible explanation of this shift could be the effect of the 0.5 mm aluminum scan horn window which the electron beam passed through before striking the samples. If the window thickness is added to the material thickness of the experimental measurements, the peak dose position would be shifted toward greater depths and would account for about half of the difference observed between the peak positions of the experi-

TABLE 6

Comparison of Experimental and Calculated Depth-Dose Parameters for Carbon and Aluminum

Ratio of Experimental to Calculated Values*

	X_p	R_e	D_p/D_e
Carbon	0.826	0.953	0.986
Aluminum	0.936	0.954	0.863

Note:* Experimental values used are averages of "stack", "wedge", and both film types from Tables 3 and 4. Calculated values are derived from results of Berger and Seltzer [23] shown in Figure 13. Symbols used are the same as for the previous tables.

mental and calculated curves. Two other effects could cause a shift in the experimental curves relative to the calculated results: (1) the electron beam energy could be degraded to lower energies because of its passage through the scan window, and (2) the electron beam could have been not normal, having a significant divergence at the entrance to the irradiated medium. Neither of the last two effects would appear to be significant; however, more measurements are required to establish with confidence these depth-dose distributions.

The experimental results strongly suggest that the "wedge" method is equivalent to the "stack" method for measuring depth-dose distributions. In principle, for normal incidence of the electron beam, the "stack" method is a more favorable geometrical arrangement of the dosimeters and medium than the "wedge" method in which a possibility exists for "channeling" of some of the electrons in the gaps between the strip of dye-film dosimeter and the medium. However, since the results show that "channeling" is not a problem, the "wedge" is superior for most applications because it allows continuous high-resolution measurement of the energy-deposition profiles as well as greatly reducing the time and effort required to handle and read the dosimeters.

D.2. Comparison of Nominal and Experimental Entrance Doses

Irradiation doses for the various materials were specified initially as nominal entrance doses in water which were based on previous measurements of the linac beam with a water calorimeter [27]. Comparisons of the nominal and experimental entrance doses in water, the latter being determined from the doses measured for the various materials, are shown in Table 7. The experimental entrance dose for water, D_w, is given

Table 7

Entrance Dose in Water From Experimental Dose in Media: Comparison of Experimental and Nominal Entrance Doses

Material	Stack-S Wedge-W	D'_w (Mrad)	D_e (Mrad)	$s_{w/m}$	D_w (Mrad)	D_{w/D'_w} *
		Film Type A				
Carbon	S	1.0	1.06	1.136	1.20	1.20
	W	1.0	1.06	1.136	1.20	1.20
Aluminum	S	1.0	1.19	1.222	1.45	1.45
	W	1.0	1.18	1.222	1.44	1.44
Polyethylene	S	1.5	1.58	0.973	1.54	1.03
	W	1.5	1.57	0.973	1.53	1.02
Polysytrene	S	1.5	1.59	1.035	1.65	1.10
	W	1.5	1.43	1.035	1.48	0.99
		Film Type B				
Carbon	S	2.0	1.71	1.136	1.94	0.97
	W	2.0	2.08	1.136	2.36	1.18
Aluminum	S	2.0	1.86	1.222	2.27	1.14
	W	2.0	1.74	1.222	2.13	1.06
Polyethylene	S	2.0	1.89	0.973	1.84	0.92
	S	2.0	2.17	0.973	2.11	1.06
Polystyrene	S	2.0	1.88	1.035	1.95	0.98
	W	2.0	2.00	1.035	2.07	1.04

*Symbols are as follows:

D'_w is the nominal entrance dose in water which was based on previous measurements of the linac beam with a water calorimeter [27];

D_e is the experimental entrance dose in the specified material;

$s_{w/m}$ is the mass collision stopping power ratio of water to the material at 10 MeV;

D_w is the experimental entrance dose in water.

by modifying Equation (2) to be

$$D_w = s_{w/m} \cdot D_e \tag{7}$$

where $s_{w/m}$ is the mass collision stopping power ratio of water to the material at 10 MeV, and D_e is the experimental entrance dose in the specified material. Examination of the ratios of the experimental to nominal entrance dose, D_w/D'_w, indicates that the nominal dose was correctly specified in most cases with the exception of irradiations in carbon and aluminum for film type A and the carbon "wedge" and aluminum "stack" for film type B.

D.3. Comparison of Tissue and Near Tissue-Equivalent Materials

In an effort to determine which of the two high polymer materials used in this study is closest to tissue in its energy-absorption properties, a comparison is made of some of the depth-dose parameters of the materials for 10-MeV electrons as shown in Table 8. The parameters for tissue are taken to be those for muscle as calculated by Berger and Seltzer [24]. It appears that there is no clear preference for one polymer material over the other as far as being tissue equivalent. The polystyrene values are slightly higher than muscle for the range and depth of peak parameters while the polyethylene values are slightly lower. The inverse is true for the stopping power values. Both materials have values within 5 percent of the values for muscle. If measurements were made with both materials, interpolation between values obtained should give results close to tissue. However, as can be seen in Table 8, water is much closer in electron energy-absorption properties than either of the polymer materials.

Table 8

Experimental and Calculated Depth-Dose Parameters of Tissue and Near Tissue-Equivalent Materials for 10-MeV Electrons

Material	Range (g/cm^2)	Depth of Peak Dose (g/cm^2)	Mass Collision Stopping Power ($MeV \cdot cm^2/g$)
Muscle	4.939 (a)	——	1.978 (a)
Water	4.880 (a)	2.83 (b)	2.000 (a)
Polystyrene	5.095 (a)	3.00 (c)	1.932 (a)
	5.13 (c)		
Polyethylene	4.792 (a)	2.73 (c)	
	4.99 (c)		

(a) Calculated, Berger and Seltzer [24].

(b) Calculated, Berger and Seltzer [28].

(c) Experimental, this report.

D.4. Possible Negative Effects on Results by Some Experimental Conditions

As discussed in Section C.3., a defect existed in the polyethylene "wedge" assembly which could have caused unreliable results. This was a result of improper machining of the two halves of the wedge, thereby making possible an air gap between the polyethylene and the dye-film dosimeter if the two parts of the wedge were not held together tightly during assembly. Also, a discharge which occurred in one of the polystyrene blocks during irradiation could have caused additional coloration to the dye-film dosimeters in that assembly. Such a discharge happened only once in the four irradiations made of polystyrene assemblies and did not occur during any of the irradiations of other materials.

Another adverse experimental condition was the thermal heating of the blocks of material upon and immediately after irradiation. Temperature dependence studies of the two types of dye-film dosimeters have been made with the films held at constant temperatures during ^{60}Co γ-ray irradiations [12-14]. Under these conditions, film type A displays a positive temperature coefficient; that is, the response to radiation increases with increasing temperature. On the other hand, film type B exhibits a negative temperature coefficient above room temperature under these conditions. If the dosimeters behaved in this way during the electron beam irradiations, the difference between the responses of the two types of dosimeters should have been as great as 40% at the peak dose for the carbon measurements. However, comparison of the peak-to-entrance dose ratios in Table 4 for the different dosimeters shows agreement to within 5 percent. In addition, previous dose-rate studies [11] of film type B indicate no significant temperature dependence for fast-pulse electron irradi-

ations where the temperature reached 30°C above room temperature but cooled to near room temperature in less than 10 seconds. Hence, thermal heating by electron beams, where the total dose is delivered in a short time, does not seriously affect the response of these dosimeters.

D.5. Suggestions for Future Experiments

Since the experiments described in this report were primarily designed to enable the Natick Laboratories to better understand the total energy deposited and the energy-depositions profiles in irradiated food products, it would be desirable to perform additional experiments using the dye-film dosimeters in actual meat packages during irradiation. For these irradiations, the dosimeters should be used in the bulk of the meat (preferably in a "wedge" configuration) as well as perpendicular to the electron beam near the interface of the meat and its package. Such experiments would give basic data which are relevant to energy deposition in tissue. Also, these measurements would demonstrate more exactly how energy is deposited in the food products under processing conditions; that is, the effects of boundaries especially would be accounted for. Furthermore, comparisons of measurements with the Monte Carlo calculated predictions could be made in order to verify the applicability of these calculations in a wide variety of similar irradiations.

REFERENCES

1. Burlin, T.E., Cavity-Chamber Theory, Radiation Dosimetry, Vol. 1, Attix and W.C. Roesch, Eds., Academic Press, New York, p.332(1968).
2. McLaughlin, W.L., Hussman, E.K., The Measurement of Electron and Gamma-Ray Dose Distributions in Various Media, Large Radiation Sources and Accelerators in Industrial Processes, IAEA, Vienna, p. 579 (1969).
3. Eisen, H., Rosenstein, M., and Silverman, J., Electron Dosimetry Using Chalkley-McLaughlin Dye-Cyanide Thin Films, Dosimetry in Agriculture, Industry, Biology, and Medicine, IAEA, Vienna, p. 615 (1973).
4. Rosenstein, M., Eisen, H., and Silverman, J., Electron Depth-Dose Distribution Measurements in Finite Polystyrene Slabs, J. Appl. Phys. 43, 3191 (1972).
5. Eisen, H., Rosenstein, M., and Silverman, J., 2.00-MeV Electron Depth-Dose Measurements in Aluminum, Copper, and Tin Absorbers Using a Radiochromic Dye Film, Intern. J. Appl. Rad. Isotopes 23, 97 (1972).
6. Eisen, H., Rosenstein, M., and Silverman, J., Electron Depth-Dose Distribution Measurements in Two-layer Slab Absorbers, Rad. Res. 52, 429 (1972).
7. Hussman, E.K. and McLaughlin, W.L., Dye Films and Gels for Megarad Dosimeters, Radiation Dose and Dose Rate Measurements in the Megarad Range, National Physical Laboratory, Teddington, England, p. 35 (1970).

8. McLaughlin, W.L., Radiochromic Dye Cyanide Dosimeters, Manual on Radiation Dosimetry, N.W. Holm and R.J. Berry, Eds., Marcel Dekker, Inc., New York, p. 377 (1970).

9. Harrah, L.A., Chemical Dosimetry with Doped(halostyrene) Film, Radiation Research 41, 229 (1970).

10. Harrah, L.A., Stored Charge Effects on Electron Dose-Depth Profiles in Insulators, Appl. Phys. Letters 17, 421 (1970).

11. Chappell, S.E. and Humphreys, J.C., The Dose-Rate Response of a Dye-Polychlorostyrene Film Dosimeter, IEEE Trans. Nucl. Sci. NS-19, 175 (1972).

12. Bishop, W.P., Humpherys, K.C., and Randtke, P.T., Poly(halo)styrene Thin-film Dosimeters for High Doses, Rev. Sci. Instr. 44, 443(1973).

13. Humpherys, K.C. and Wilcox, R.L., Radiochromic Dosimetry and Rate Effects, EG&G Report No. 1183-2218 (1969).

14. Humpherys, K.C. and Randtke, P.T., Doped Poly(halo)styrene Dosimeter Materials Studies, EG&G Report No. 1183-2267 (1971).

15. Frankhauser, W.A., Measurement of the Radiation Response of a Radiochromic Dosimeter Exposed to a Pulsed Electron Beam Source, EG&G Report 1183-5024 (1973).

16. Brynjólfsson, A. and Thaarup, G., Determination of Beam Parameters and Measurements of Dose Distribution in Materials Irradiated by Electrons in the Range of 6 MeV to 14 MeV, Danish AEC, Risö Report No. 53 (1963).

17. Bishop, W.P. and Benson, J.L., Operational Treatment of Multiple Reflection Interference in the Readout of Thin-film Poly(halo)styrene Dosimeters, Sandia Laboratories Report No. SC-DR-72 0641(1972).

18. Petree, B. and Lamperti, P., A Comparison of Absorbed Dose Determinations in Graphite by Cavity Ionization Measurements and by Calorimetry, J. of Research Natl. Bur. Stnds. 71C, 19 (1967).

19. Weiss, J. and Rizzo, F.X., Cobalt-60 Dosimetry in Radiation Research and Processing, Manual on Radiation Dosimetry, N.W. Holm and R. J. Berry, Eds., Marcel Dekker, Inc., New York, p. 231 (1970).

20. Evans, R.D., X-Ray and γ-ray Interactions, Radiation Dosimetry, Vol. 1, F.H. Attix and W.C. Roesch, Eds., Academic Press, New York, p. 93 (1968).

21. Chan, F.K. and Burlin, T.E., An Experimental Examination of a General Cavity Theory Using a Solid State Dosimeter, Br. J. Radiol. 43, 54 (1970).

22. McLaughlin, W.L., Hjortenberg, P.E., and Radak, B.B., Absorbed-Dose Measurements With Thin Films, Dosimetry in Agriculture, Industry, Biology and Medicine, IAEA, Vienna, p. 577 (1973).

23. Berger, M.J. and Seltzer, S.M., private communication.

24. Berger, M.J. and Seltzer, S.M., Tables of Energy Losses and Ranges of Electrons and Positrons, NASA SP-3012 (1964) and SP-3036 (1966).

25. Pages, L., Bertel, E., Joffre, H., and Sklavenitis, L., Energy Loss, Range, and Bremsstrahlung Yield for 10-keV to 100-MeV Electrons in Various Elements and Chemical Compounds, Atomic Data 4, (1)1(1972).

26. Katz, L. and Penfold, A.S., Range-Energy Relations for Electrons and the Determination of Beta-Ray End-Point Energies by Absorption, Revs. Mod. Phys. 24, 28 (1952).

27. Holm, N.W. and Jarrett, R.D., An Evaluation of Dosimetry Procedures Applicable for Use in Food Irradiation, Nat. Acad. of Science, Nat. Research Council, Publication 1273, 361 (1965).

28. Berger, M.J., and Seltzer, S.M., Calculation of Energy and Charge Deposition and of the Electron Flux in a Water Medium Bombarded with 20-MeV Electrons, Annals New York Academy of Sciences 171, Art. 1, 8 (1969).

NBS-114A (REV. 7-73)

U.S. DEPT. OF COMM. BIBLIOGRAPHIC DATA SHEET	1. PUBLICATION OR REPORT NO. NBSIR 73-413	2. Gov't Accession No.	3. Recipient's Accession No.

4. TITLE AND SUBTITLE

Measurement of Depth-Dose Distributions in Carbon, Aluminum, Polyethylene, and Polystyrene for 10-MeV Incident Electrons

5. Publication Date: November 1973

6. Performing Organization Code

7. AUTHOR(S)
J.C.Humphreys, S.E. Chappell, W.L. McLaughlin, & R.D. Jarrett

8. Performing Organ. Report No. NBSIR 73-413

9. PERFORMING ORGANIZATION NAME AND ADDRESS

NATIONAL BUREAU OF STANDARDS
DEPARTMENT OF COMMERCE
WASHINGTON, D.C. 20234

10. Project/Task/Work Unit No. 2430411

11. Contract/Grant No. AMXRED 73-141

12. Sponsoring Organization Name and Complete Address *(Street, City, State, ZIP)*

Food Laboratory
U.S. Army Natick Laboratories
Natick, Massachusetts 01760

13. Type of Report & Period Covered: Interim Report

14. Sponsoring Agency Code

15. SUPPLEMENTARY NOTES

16. ABSTRACT *(A 200-word or less factual summary of most significant information. If document includes a significant bibliography or literature survey, mention it here.)*

Depth-dose distributions of 10-MeV electrons incident on homogeneous media of carbon, aluminum, polyethylene, and polystyrene have been measured using thin radiochromic dye-film dosimeters. Two types of dye-film dosimeters were employed as "cavities" within the media in two different geometrical configurations. One configuration was a stack with the dosimeters interleaved between disks of the medium and placed perpendicular to the incident electron beam direction. The other configuration was a wedge assembly with a single piece of dye film placed between pieces of the medium at a small angle to the beam direction. The results show no significant difference between dosimeter type or experimental arrangement. In addition, good agreement is shown in comparisons of experimental and Monte Carlo calculated depth-dose distributions characterized by such parameters as extrapolated range, depth of peak dose, and ratio of peak to entrance dose.

17. KEY WORDS *(six to twelve entries; alphabetical order; capitalize only the first letter of the first key word unless a proper name; separated by semicolons)*

Aluminum; carbon; depth dose; depth-dose distributions; dye-film dosimeters; polyethylene; polystyrene; radiochromic dyes; 10-MeV electrons

18. AVAILABILITY

[X] Unlimited

[ ] For Official Distribution. Do Not Release to NTIS

[ ] Order From Sup. of Doc., U.S. Government Printing Office Washington, D.C. 20402, SD Cat. No. C13

[ ] Order From National Technical Information Service (NTIS) Springfield, Virginia 22151

19. SECURITY CLASS (THIS REPORT): UNCLASSIFIED

21. NO. OF PAGES: 54

20. SECURITY CLASS (THIS PAGE): UNCLASSIFIED

22. Price

AMERICAN REVOLUTION BICENTENNIAL
1776-1976